REPORT DOCUMENTATION PAGE

Form Approved
OMB No. 0704-0188

ATE	3. REPORT TYPE AND DATES COVERED
	Reprint 7/1/92 - 12/31/92

4. TITLE AND SUBTITLE

Fundamental aspects of brittle cooperative phenomena - Local load sharing models

5. FUNDING NUMBERS

(2)

DAAL03-91-G-0030

6. AUTHOR(S)

Dusan Krajcinovic and Dragoslav Sumarac

7. PERFORMING ORGANIZATION NAME(S) AND ADDRESS(ES)

Arizona State University
Tempe, Arizona 85287

8. PERFORMING ORGANIZATION REPORT NUMBER

9. SPONSORING/MONITORING AGENCY NAME(S) AND ADDRESS(ES)

U. S. Army Research Office
P. O. Box 12211
Research Triangle Park, NC 27709-2211

10. SPONSORING/MONITORING AGENCY REPORT NUMBER

ARO 28222.4-EG

11. SUPPLEMENTARY NOTES

The view, opinions and/or findings contained in this report are those of the author(s) and should not be construed as an official Department of the Army position, policy, or decision, unless so designated by other documentation.

12a. DISTRIBUTION/AVAILABILITY STATEMENT

Approved for public release; distribution unlimited.

12b. DISTRIBUTION CODE

13. ABSTRACT *(Maximum 200 words)*

The present paper considers the effect of stress concentrations on the damage evolution in brittle solids with disordered microstructure. This problem is herein approached studying discrete models provided with a local load sharing rule. Two of these models: tight bundle parallel bar model and lattices, are employed to establish universal trends in brittle cooperative deformation processes.

14. SUBJECT TERMS

Damage mechanics, rupture, stress concentrations

15. NUMBER OF PAGES

16. PRICE CODE

17. SECURITY CLASSIFICATION OF REPORT	18. SECURITY CLASSIFICATION OF THIS PAGE	19. SECURITY CLASSIFICATION OF ABSTRACT	20. LIMITATION OF ABSTRACT
UNCLASSIFIED	UNCLASSIFIED	UNCLASSIFIED	UL

Mechanics of Materials 15 (1993) 117–129
Elsevier

Fundamental aspects of brittle cooperative phenomena – Local load sharing models

Dusan Krajcinovic and Dragoslav Sumarac [1]

Mechanical and Aerospace Engineering, Arizona State University, Tempe, AZ 85287-6106, USA

Received 13 March 1992; revised version received 3 November 1992

The present paper considers the effect of stress concentrations on the damage evolution in brittle solids with disordered microstructure. This problem is herein approached studying discrete models provided with a local load sharing rule. Two of these models: tight bundle parallel bar model and lattices, are employed to establish *universal* trends in brittle cooperative deformation processes.

1. Introduction

The stress concentration attributed to the presence of microcracks and microvoids is commonly regarded as one of the leading causes of failure in materials. As a result of the defect induced stress concentration material adjacent to the existing microdefect is much more likely to fail than the undamaged regions far from the defect subjected to average, or far field stresses. Consequently, a rigorous analysis of the cooperative brittle phenomena must consider spatial distributions of strengths and stresses. In contrast to the loose bundle parallel bar model (considered in the first part of this study, Krajcinovic et al. (1993)) it is, thus, necessary to consider not only the statistical distribution of rupture strengths but also the precise locations of weak links within the system. This problem is obviously much more difficult since it involves a more complete description of the microstructural disorder.

Correspondence to: Prof. D. Krajcinovic, Department of Mechanical and Aerospace Engineering, College of Engineering and Applied Sciences, Arizona State University, Tempe, AZ 85287-6106, USA.

[1] Permanent address: Civil Engineering Department, University of Belgrade, Yugoslavia.

The proposed strategy is to extract simple, universal trends and features of the macro response through considerations of simplified network models emphasizing disordered microstructures. The universality should be understood as a property invariant of the details (higher statistical momenta) of the disorder, damage evolution, etc. Once determined, universal parameters and trends, being common to an entire class of materials and phenomena, will greatly facilitate formulations of more sophisticated models necessary for application in engineering design.

2. Parallel bar model

In general, a local load sharing rule may be introduced rigorously through a more sophisticated discretization or in a simpler, but more arbitrary, manner using a modified version of the parallel bar model allowing for unequal distribution of loads released by the ruptured link. To establish connection with the preceding study it seems reasonable to consider first the latter alternative. In a parallel bar model a local load sharing rule may be postulated a priori (directly) or by means of a hierarchical grouping of links into cells.

0167-6636/93/$06.00

2.1. Parallel bar model with local load sharing

Fluctuations of forces within a parallel bar model can be, for example, estimated using an a priori selected load sharing rule. For example, Harlow and Phoenix (1982) assumed that the force released by a rupturing link is equally shared by its nearest neighbors. Even with such a simple approximation of the reality rigorous analyses turn out to be all but trivial. In fact Harlow and Phoenix (1982) were only able to derive a conservative, lower bound on the system strength assuming that the failure will occur when the two adjacent links in the bundle rupture. This assumption may be, indeed, warranted in the case of very homogeneous materials. In most structural materials, with a larger scatter in rupture strengths, macro failure is typically preceded by the formation of much larger clusters of ruptured links. Unfortunately, "the complexity (*of these statistical models*) grows enormously with increasing bundle size and simplification techniques are by no means obvious" (Phoenix, 1978).

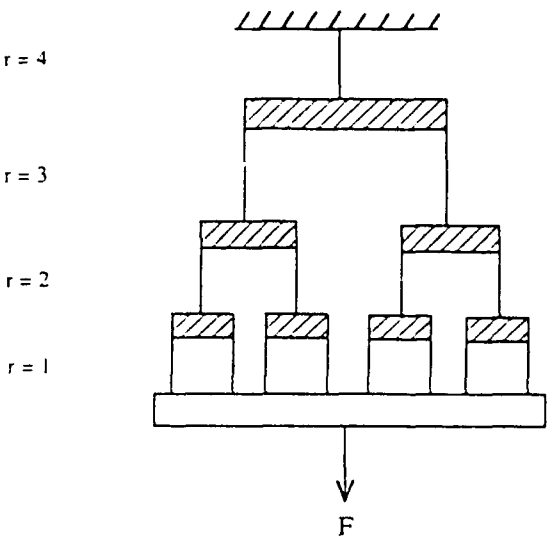

Fig. 1. A parallel bar model in form of a Cayley tree of functionality two.

2.2. Hierarchical models

In many cases natural systems and materials, such as tendons (Cassidy et al., 1990), are intrinsically hierarchical. In other cases, the self-similarity on several scales is the product of manufacturing processes (solidification) or non-equilibrium growth (vapor deposition). Finally, the scale invariance may also be the consequence of the stress directed dilution of common materials with disordered microstructure. Indeed, measurements indicate that the failure surfaces caused by fracture (Mandelbrot et al., 1984), faulting and microcrack growth and coalescence are characterized by fractal geometry. Hence, the study of hierarchical structures may be important both for their own sake and as an approximation of the local load sharing rule.

A hierarchical structure studied by Smalley et al. (1985) is topologically a Cayley tree shown in Fig. 1. The original parallel bar model (bottom level in Fig. 1) containing N links is partitioned into $N/2$ cells, each containing two links. The rupture strengths of individual links are distributed according to an appropriately selected rupture strength distribution function $p(f_r)$. The spatial distribution of links with unequal strength is typically varied to study the effect of different realizations of the same statistics.

Initially, all links carry identical loads $f = F/N$, where F is the externally applied tensile load. When a link ruptures the force it carried is released and quasi-statically transferred to the remaining link in the cell. A cell fails only if both constituent links rupture. Consequently, the failure of a cell of order (r) represents the rupture of a corresponding link of the order $(r+1)$ (see Fig. 1). In this sense, the hierarchical, Cayley tree, model introduces a simplified load sharing rule. More realistic load sharing rules may be formulated by increasing the number of links in a cell (functionality) at the expense of the simplicity and tractability.

The transfer of forces within the Cayley tree was quantified by Smalley et al. (1985) introducing conditional probabilities defining the chance that a cell will fail when the force from a ruptured link is transferred within the same cell to

the extent link. Omitting the details of the derivation, available in Smalley et al. (1985) and Herrmann and Roux (1990), it suffices for present purposes to list the final recursive expression relating cumulative (Weibull) probabilities of failure $P(f_r)$ in cells of two sequent orders (r) and $(r+1)$,

$$P^{(r+1)} = 2P^{(r)}\left[1 - (1 - P^{(r)})^4\right] - (P^{(r)})^2. \qquad (1)$$

In this particular case, the cumulative probability function $P(f > f_r)$, i.e., the maximum force which can be entrusted to the considered hierarchical system, can be solved from (1) by iteration. Instead, Smalley et al. (1985) applied the renormalization group method according to which the failure corresponds to the bifurcation (or unstable fixed) point in the $(P^{(r)}, P^{(r+1)})$ space. For the Weibull rupture strength distribution (Eq. (2.11) in Part I) (with the shape parameter $\alpha = 2$) the bifurcation point corresponding to the recursive equation (1) is $P^* = 0.2063$. For $P < P^*$ the solution tends to $p = 0$ (stable state), while for $P > P^*$ the solution of (1) tends to $p = 1$ (rupture).

The corresponding value of the maximum force is then $F_m = 0.4807\sqrt{2}\ Ku_+ = 0.6798\ Ku_m$ (where u_+ and u_m are the Weibull scale parameter and the system displacement at maximum force $F = F_m$). In comparison, the loose bundle (equal load sharing) estimate for the same distribution of rupture strengths can be computed from Eq. (2.13) in Part I as $F_m = e^{-1/2}\ Ku_m = 0.6065\ Ku_m$. The difference of 11% between these two estimates is obviously a direct result of the selected load sharing rule (i.e., cell size). As expected with the increasing cell size the influence of the stress concentration is diminished. According to the numerical computations for the Cayley tree having cells containing four links (approximating a two-dimensional parallel bar model) $F_m = 0.4327\ Kx_+ = 0.6119\ Ku_m$ which is only 1.3% in excess of the loose bundle estimate. This result provides a first but nevertheless convincing evidence that the direct interaction of defects has a second-order effect on the system response during the precritical stage of the deformation process and the magnitude of the maximum force F_m itself.

3. Lattices

On the next level of sophistication a solid may be partitioned into irregular polyhedra ("finite elements") referred to as Voronoi tessellation (froth) or Wigner–Seitz cells. Cellular representation of solids, which predates discretizations such as finite elements, are natural and common in modeling stochastically nonuniform solids with disordered microstructure. Dual to this division into cells is the Delauney simplicial graph (network, see Zallen (1983) and Ostoja-Starzewski and Wang (1989)) shown in Fig. 2. The sides of the original Voronoi polyhedra ("finite elements") are orthogonal to the bonds (sides) of the Delauney network (lattice). The nodes of the simplicial Delauney network are equidistant from the point of intersection of two graphs. The attribute "simplicial" refers to the fact that the Delauney division consists of simplest polyhedra (triangles in two and tetrahedra in three dimensions) or simplexes. It can be shown that the Voronoi polyhedra and Delauney simplexes can fill the entire space.

In a manner analogous to one suggested by Englman et al. (1984) it will be assumed that the load carrying capability of a Voronoi "finite element" is exceeded in a given direction when the bond of the dual Delauney graph in that direction ruptures. In this sense the considered discretization is a generalization of the "local approach to fracture" concept introduced by

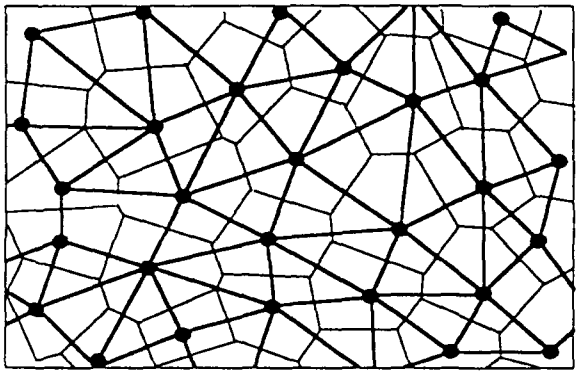

Fig. 2. Voronoi polyhedra and its dual Delauney network (bold lines).

Lemaitre (1986) and successfully applied in finite-element computations thereafter.

Introducing Delauney network a two-dimensional continuum is approximated by an articulated network of links joined at nodes. The nodes may form a periodic lattice of regular geometry or an irregular, topologically disordered, Delauney network. Structurally, a lattice or a network may be either a truss (central-force lattice) or a grid (frame). The links of a truss are subjected only to axial forces. The elements of a grid can support both axial forces and bending moments preventing relative rotations of links in a node. With respect to the connectivity range a node may be connected only to the nearest neighbors (nodes forming the first coordination group – simple trusses) or nodes of several coordination groups (complex trusses). The present study will concentrate only on some of the many possible alternatives obtained combining features mentioned above. In particular only the planar lattices having perfect, periodic, geometry will be considered in the sequel.

The lattice models to be discussed within this study should not be confused with the geometrically similar models used in molecular dynamics problems. Present study considers lattices only as elementary discretizations of solids allowing for simple analyses. In the case of molecular dynamics models nodes actually represent the molecules or atoms. Thus, the intermolecular (bond) forces must be derived from the interaction energy typically approximated by the "Lenard–Jones 6–12 potential".

3.1. Percolation models

In view of the substantial literature on the percolation theory (see Stauffer, 1985, etc.) a short précis of basic aspects will suffice to render the following discussion at least partially self-contained. Only the bond percolation problem will be considered and p will denote the probability that a link is present (and $q = 1 - p$ that the bond is absent or ruptured). In its initial state of quenched disorder a lattice is usually weakened by few missing links randomly distributed over the entire lattice. The lattice is subsequently diluted by sequential removal of links which can be either random or directed by applied loads (postulating an appropriate rupture criterion). In the course of a dilution process the number of missing links grows along with the probability of emergence of larger, irregularly shaped clusters of missing links. Coincidentally, the stiffness of the lattice decreases. At the elastic percolation threshold $p = p_{ce}$ the stiffness of the lattice is reduced to zero. At this point the initial state characterized by a disordered distribution of defects abruptly makes a transition into a state dominated by a single, highly localized cluster of missing links. At the percolation threshold a transition takes place from defects characterized by short-range connectivity to a defect cluster exemplifying long-range connectivity (localization). The infinite (spanning) cluster emerging at $p = p_{ce}$ transects the infinite lattice. The percolation thresholds p_{ce} available in the literature pertain to lattices of infinite sizes. Numerical simulations are, however, for obvious reasons performed on large but finite lattices. The effect of the finite size is, subsequently, eliminated by finite-size scaling.

The considered dilution process is characterized by a continuous and gradual change of the microstructure (number of extent links) which at the elastic percolation threshold results in an abrupt, qualitative change of the response reflected in the singularity of the system compliance. A phenomenon of this type is commonly referred to as the phase transition. As in the case of the parallel bar model the Gibbs energy remains continuous (Krajcinovic et al., 1993) while its second derivative with respect to the force becomes singular at $p = p_{ce}$. Consequently, the considered critical phenomenon (change in the connectivity range) is a second-order phase transition. Finally, in the proximity of the percolation threshold the lattice stiffness (or less rigorously the elastic modulus on the macro-scale) changes slowly with the proximity parameter $(p - p_c)$ before vanishing at $p = p_c$. Hence, the lattice stiffness is a reasonable candidate for the order parameter.

The most remarkable aspect of the percolation theory is that the systems belonging to the same

universality class have identical asymptotic behavior in the vicinity of the critical state. More specifically, the systems (phenomena) forming a universality class have identical percolation thresholds p_c and scaling laws defining the rate of change of the transport properties in the proximity of the percolation threshold. While the percolation threshold depends only on the dimensionality d and the lattice type (microstructure), the scaling law for the stiffness and other parameters exhibiting singular behavior as $p \to p_c$ depends only on the dimensionality d.

In its conventional form the percolation model recognizes only two alternatives; a link is either missing (or ruptured) with a probability $q = 1 - p$, or is present with a probability p. All links are assumed to have identical cross sectional area A and elastic modulus E. The elastic energy of the lattice is (modifying slightly the expression from Hansen, 1990)

$$2V = EA \sum_{ij} L^{-1} g_{ij} \left[(u_i - u_j) \cdot e_{ij} \right]^2 + EI \sum_{ij} L^{-3} g_{ij} g_{ik} \theta_{ijk}^2, \tag{2}$$

where u_i is the displacement of the node i, e_{ij} a unit vector located at node i and directed towards the node j and θ_{ijk} the change of angle between the links ij and ik. Also, I is the modulus of inertia and L the length of a link. Finally, $L^{-1} g_{ij} = L^{-1}$ if the link is present and zero otherwise.

3.1.1. Central-force lattices (trusses)

The simplest models ensue neglecting the link bending stiffness (EI/L^3) and reducing expression (2) to the first of the two terms on the right-hand side. The mean-field theory estimate for the central-force lattice stiffness and the percolation threshold for a random dilution can be determined in a very simple manner. If N is the number of nodes, the number of degrees of freedom is then (Nd) where d is the lattice dimensionality. If z denotes the coordination number (i.e., number of links at each node) then the total number of constraints is ($zNp/2$). During a random dilution process a truss becomes statically determinate when the number of constraints equals the number of degrees of freedom, i.e., when

$$p = p_{cen} = 2d/z. \tag{3}$$

Removal of a single additional link beyond the percolation limit (3) transforms the truss into a mechanism unable to support externally applied loads. In (3) the subscript (cen) refers to the elastic percolation threshold for a central-force lattice.

During the initial phase of the process the number density p of extant links is well above the percolation limit p_{cen}. During this phase of the deformation process the missing links (defects), scattered over the lattice, are far from each other. Forces in the links are almost equal to corresponding forces in the pristine lattice rendering the self-consistent theory applicable. Consequently, the lattice stiffness is during this phase a linear function of p. Thus, the mean-field estimate for the tangent stiffness of a randomly diluted central-force lattice is

$$\frac{K_T}{K} = \frac{p - p_{cen}}{1 - p_{cen}} = \frac{1}{z - 2d}(zp - 2d), \tag{4}$$

where K is the stiffness of the undamaged (pristine) lattice for which $p = 1$.

Numerical simulations by Feng and Sen (1984), Sahimi and Goddard (1986), Beale and Srolovitz (1988) and others on diluted triangular two-dimensional central-force lattices lead to several important conclusions. In all cases the linear self-consistent region (4) persisted to surprisingly small tangent stiffnesses ($K_T \approx 0.05K$). The cross-over region connecting the mean-field and percolation regimes was, consequently, very short. Within numerical errors the percolation threshold was found to be $p_{cen} \approx 0.65$ which for $z = 6$ (triangular lattice) is closely fitted by the mean-field estimate (3) according to which $p_{cen} = 2(2)/6 = 2/3$.

A complete analysis of a large central-force triangular lattice having 14,700 bonds was per-

formed by Beale and Srolovitz (1988) who estimated the percolation threshold (i.e., the density of existing bonds at the instant of vanishing macro stiffness) as $p = p_{cen} = 0.65 \pm 0.005$. The force–displacement curve of the considered lattice, subjected to tensile tractions at two ends, was found in form of a number of sharp spikes separated by stretches during which the displacement increases at zero force. This, physically meaningless, response is attributable to the loss of internal stability of the truss and subsequent rigid body pivoting of the overconstrained segments of the truss needed to align the extant links with the externally applied forces. This instability is the consequence of the vectorial nature of the equilibrium equations for a lattice node and is, in fact, not present in conduction phenomena.

Literature focused on the elastic percolation problems is vague on a rather crucial issue. Almost as a rule the overall (lattice or specimen) stiffness is confused with the elastic modulus. Even more importantly it is not obvious whether the scaling law pertains to the tangent or secant stiffness and whether the percolation threshold is defined as a dilution level at which the tangent stiffness K_T or the secant stiffness K reduces to zero. All experiments (Benguigui, 1984; Sieradzki and Li, 1986; Benguigui et al., 1987) reported in the literature were load controlled. Since the post-peak (softening) segment of the force–displacement curve is unstable a load controlled test cannot distinguish between $K = 0$ and $K_T = 0$.

The arguments in the first part of this study (Krajcinovic et al.,. 1993) indicate that the phase transition occurs at the apex of the force–displacement curve, i.e., when $K_T = 0$. However, the infinite cluster emerges at this point only in force controlled cases. On purely physical grounds it is appealing to conjecture that the onsets of change in connectivity (percolation threshold), localization, loss of homogeneity in displacement field and loss of ellipticity of the governing equations are different manifestations of the same phenomenon (criticality). However, this issue can be settled conclusively only by precise force and displacement controlled tests which, to the best knowledge of the authors, were not as yet reported in the literature.

3.1.2. Frames (grids)

Two major problems associated with the central-force lattice model are: (a) occurrence of the model incured instabilities; and (b) the fact that the elastic percolation threshold p_{cen} significantly exceeds the percolation threshold p_c for the conductivity problems. The physics and mathematical structure of the conductivity and elastic percolation problems are by no means identical. The Kirchhoff equations defining the partition of electric current in a node are scalar in contrast to the nodal equilibrium equations which are vectorial. However, in two-dimensional problems two percolation thresholds should coincide since the cluster of missing links traversing the lattice (p_c) transects it as well (p_{ce}) (Krajcinovic and Basista, 1991). To illustrate the role of the internal instabilities it suffices to examine a square or cubic lattice. Since neither of these two lattices, even when all links are present, has any shear stiffness their percolation threshold is $p_{cen} = 1$ (as observed in Roux and Guyon, 1985).

There are at least two ways in which the situation can be remedied. Firstly, the local instabilities can be prevented constraining relative rotations of links in nodes assuming built-in conditions at each node and endowing the links with bending rigidity. Alternatively, each node can be connected to nodes belonging to more than one coordination group to reduce the chance for the occurrence of internal instabilities. At this point only the first of these two alternatives will be examined.

Determination of the elastic percolation threshold p_{ce} for a grid necessitates extensive numerical simulations. According to the results of simulations reported in Kantor and Webman (1984), Feng et al. (1985), Sahimi (1986) and others, it turns out that for a grid $p_{ce} \approx p_c$. Thus, as expected on purely geometric grounds, elastic and conductivity percolation thresholds (once the internal instabilities are eliminated) are indeed identical. This facilitates application of the percolation theory in mechanics since the conductivity percolation thresholds for several different periodic lattices are available in Stauffer (1985) and other standard monograph on the percolation theory. The effect of the rotational constraints in

lattice nodes is very significant. For example, the fraction of bonds needed to maintain the load carrying capability is lowered from 0.645 to 0.347 for triangular lattice and from 1.0 to 0.5 for the quadratic lattice.

Finally, an argument can be made that the regularity of the considered lattices has no effect on the conclusions. Being simplicial, a planar Delauney network has an identical coordination number $z = 6$ as the regular triangular lattices. Since the product $zp_c^b \approx 2.0 \pm 0.2$ (where the superscript b stands for bond percolation) is a dimensional invariant for all examined lattices (Zallen, 1983) it seems reasonable to conclude that the bond percolation thresholds for triangular and Delauney lattices are similar in magnitude. Consequently, the pre-peak (hardening) response of a triangular lattice is not affected by the regularity (periodicity) of the lattice. An analogous conclusion was, in the context of the sol–gel transition reached by de Gennes (1979, Ch. V.2.8).

3.1.3. Directed percolation

The above listed data are related to perfectly random dilution of lattices. In the course of random dilution processes the lattice stiffness tensor changes isotropically. A glance at the lattices studied by Beale and Srolovitz (1988) indicates that in the case of dilution processes driven by arbitrarily oriented externally applied forces (uniaxial in their case) only some of the components of the stiffness tensors become singular at the percolation threshold. The links aligned with the externally applied tractions are subjected to the largest forces and are, therefore, much more likely to fail than other links.

In the case of directed percolation infinite cluster of missing links forms in a direction roughly perpendicular to the applied tensile tractions. Therefore, it requires rupture of fewer links than necessary for random (isotropic) dilution. According to Kinzel (1983) the directed bond percolation thresholds are: $p_{cd} \approx 0.479$ for a triangular lattice and 0.6445 for a square lattice. Therefore, the Beale and Srolovitz (1988) estimate of $p_{cen} \approx 0.65$ should be compared with $p_{ced} \approx 0.479$ for directed percolation and not, as typically assumed, to $p_{ce} \approx 0.347$ for the isotropic (random dilution) case. The difference between p_{cen} and p_{ced} is attributable to the direction of applied forces, while the rest (to p_{ce}) is due to the lack of rotational constraints in nodes (i.e., internal, model induced, instabilities).

4. Distributed strength lattices

One of the basic shortcomings of conventional percolation models is inherent to the bimodal distribution of the rupture strengths of links which can be either equal to zero (initial damage) or to some positive constant f_r. In view of the discussion of the parallel bar models in the first part of this study (Krajcinovic et al., 1993) it is obvious that the band-width of the rupture strength distribution has a strong influence on the type of the response in both qualitative and quantitative sense. However, analyses of disordered lattices assembled from links having arbitrary distributed rupture strengths and stiffness require large-scale numerical simulations. First statistical studies of triangular lattices conducted by Sahimi and Goddard (1986) were directed towards investigation of the influence of different link stiffnesses and different link rupture thresholds on the lattice response. These analyses demonstrated that by changing the distribution of link rupture strengths it becomes possible to change the failure mode from one in which the spanning crack is of very regular geometry to one characterized by a spanning crack of very complex (fractal) geometry. In the first case, characterized by a narrow link strength bandwidth, the failure mode is brittle since almost all of the energy is dissipated to form the spanning crack. The failure in this relatively homogeneous material can be attributed solely to the stress concentration of a single defect of preferential geometry. In the latter case, characterized by a more substantial link strength bandwidth, a large number of links is ruptured without being the part of the spanning cluster and promoting the macro-failure. In other words, in this damage tolerant heterogeneous solid failure is preceded by significant dissipation of energy and attendant accumulation of damage.

A truly comprehensive study of triangular cen-

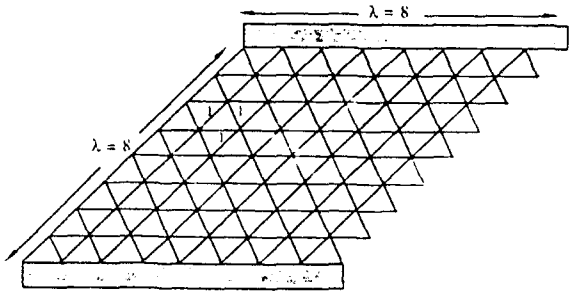

Fig. 3. A triangular lattice of size $\lambda = 8$.

tral-force lattices consisting of links with identical stiffnesses and randomly distributed rupture strengths was recently completed by Hansen et al. (1989). At each end the lattice was supplied by a rigid member (bus) ensuring identical displacement of all nodes it connects. Periodicity conditions were enforced in lateral direction to eliminate the end effects. The quenched disorder was introducing assuming uniform distribution of link rupture strengths $p(f_r) = \text{constant}$ (modeling the initial damage by links of zero strength). On such a lattice Hansen et al. (1989) performed repeated computations for a large number of different physical realizations of the same statistics. The only difference between individual simulations consisted of different spatial distribution of links strengths. To ascertain the effect of the lattice size Hansen et al. (1989) considered four different lattice sizes (with $\lambda = 4$, 8, 16 and 32 number of rows, see Fig. 3). Computations for the lattice of smallest size ($\lambda = 4$) were considered statistically unreliable since the individual defects (missing links) occupy a large portion of the lattice from the very beginning of the dilution process.

Computations were performed following the rules of conventional truss analyses. Forces in each link were computed for each external displacement increment. A link was removed and its force redistributed to extant links, in accordance with the equilibrium conditions, whenever the force in this link exceeded its strength f_r. Hansen et al. (1989) considered a symmetric rupture condition making no difference between tension and compression. However, the ensuing departure from physical reality of fracture was negligible since the considered tensile loading was not conducive to emergence of large compressive forces. Hence, since the lattice geometry was periodic, and analysis deterministic, the disorder was a direct consequence of the nondeterministic distribution of the initial damage and rupture strengths (quenched disorder).

The macro-variables defining the kinematics of the considered dissipative process are the displacement u of the lattice (change of the distance separating the rigid members) and an appropriately defined damage variable D. On micro-scale the history is recorded by the number of broken links n. Since n, or D, are the only history recording variables all macro-variables and transport properties (such as lattice stiffness) must be defined as a function of D and all micro-variables as a function of n. To determine the statistics of the process the results of computations are averaged over the entire ensemble of physical realizations selecting the number n of ruptured links as the control variable. In view of the finite size of the lattices the force–displacement relation was sought by Hansen et al. (1989) in form of the following finite-scaling Ansatz

$$F = K(1 - \sqrt{3}\,\alpha u)u. \tag{5}$$

The lattice stiffness K was, for convenience, taken to be equal to unity by Hansen et al. (1989). The parameter α was then selected to ensure the best fit between the Ansatz (5) and the computational results over the entire spectrum of parameters (lattice sizes). It was not entirely surprising that the parameter α itself was found to be a function of lattice size L. On the basis of these computations Krajcinovic and Basista (1991) proposed a simple equality

$$\alpha = \beta\lambda^{1-\beta}, \tag{6}$$

which for $\beta = 3/4$ (as suggested in Hansen et al., 1989) fits the computed data exceedingly well.

Having the above expression (6) for the parameter α the force–displacement relation can be cast in the familiar form (see part 1, Eq. (2.2)) (allowing additionally for the lattice size effect)

$$F(\lambda) = K[1 - \omega(\lambda)]u. \tag{7}$$

The damage parameter ω can be shown (for the selected uniform distribution of link rupture strengths) to be linearly proportional to the displacement u

$$\omega(\lambda) = \sqrt{3}\beta\lambda^{-\beta}u. \tag{8}$$

The damage parameter ω can be also rewritten as a function of the externally applied force F in form of

$$\omega(\lambda, F) = 0.5\left\{1 - \left[1 - 4\sqrt{3}\beta\lambda^{-\beta}(F/K)\right]^{1/2}\right\}, \tag{9}$$

where as before $\beta = 3/4$.

Similarly, the displacement corresponding to the apex of the force–displacement curve is from (7) and (8)

$$u_m = \lambda^{\beta}/2\beta\sqrt{3}, \tag{10}$$

where the subscript m denotes the value of the variable corresponding to the maximum force F_m to which the lattice can be subjected (rupture force in a load controlled test). The number of ruptured links at the apex of the force–displacement curve is

$$n_m = \lambda^{\beta+1}/2\beta. \tag{11}$$

Substitution of (10) into (8) and (7) leads to analytical expressions for the damage at the apex and maximum force which are both *independent* of the lattice size

$$\omega_m = 0.5 \quad \text{and} \quad F_m = 0.5\,Ku_m. \tag{12}$$

From (7) the secant modulus $K = K(1-\omega)$ at the apex is according to (12) equal to $0.5\,K$. The analytical expression for the number of ruptured bonds at the apex is

$$n_m = u_m\lambda\sqrt{3}. \tag{13}$$

The self-consistent estimate for the displacement can be readily derived in a manner indicated in Hansen et al. (1989). For the considered tensile loading only the diagonal links are likely to rupture. Since the total number of diagonal links is $2\lambda^2$, the damage D (number density of ruptured links) is, according to Eq. (2.3) of Part I, equal to $n/2\lambda^2$. Thus, the average strain is

$$\langle\epsilon\rangle = \epsilon_m\frac{n}{2\lambda^2}, \tag{14}$$

where ϵ_m is the strain at which the strongest link ruptures, i.e., for which $D = 1$.

At the same time since (u/λ) is the displacement of a lattice node

$$\frac{u}{\lambda} = \frac{2\langle\epsilon\rangle}{\sqrt{3}\,\epsilon_m}l, \tag{15}$$

where the length of the diagonal link l is equal to unity. Hence, the expression (13) may indeed be derived from (14) and (15) as a self-consistent estimate of the number of ruptured links at the state corresponding to the apex of the force–displacement curve.

The parameter α, number and density of ruptured links n_m, displacement u_m, force F_m and damage D_m at the apex of the force–displacement curve (failure in the stress controlled test) were computed from the above expressions and arranged in Table 1. The corresponding numerical data read off Fig. 6 in Hansen et al. (1989) are added in parentheses. As already mentioned the numerical results for $\lambda = 4$ are omitted as suggested in Hansen et al. (1989).

The remarkable accuracy with which the above expressions, derived using the simple relationship (6) for the parameter α, fit the numerical simulations provides a strong indication that the lattice

Table 1
Parameter α (Eq. (5)), number and density of ruptured bonds, displacement, force, and damage at the apex of the force–displacement curve

λ	α	n_m	n_m/N	u_m	F_m	ω_m
4	1.06 (1.00)	9	0.280	1.09	0.54	0.5 (0.500)
8	1.26 (1.25)	25 (26)	0.195	1.83 (1.91)	0.92 (0.94)	0.5 (0.521)
16	1.50 (1.50)	85 (81)	0.166	3.08 (3.00)	1.54 (1.56)	0.5 (0.487)
24	1.66 (1.65)	173 (168)	0.155	4.17 (4.13)	2.09 (2.15)	0.5 (0.495)

response during the hardening phase of the deformation process (i.e., along the ascending part of the force displacement curve) depends entirely on the volume averages of the disorder (spatial distribution of ruptured links). This is, indeed, the reason behind the close agreement between the self-consistent estimates and the results of numerical computations from Hansen et al. (1989). Moreover, since the analytical estimates of the pre-peak (hardening) segment of the response obtained by the parallel bar model are in close agreement with the numerical simulations performed on lattices the latter models should be used only when the emphasis is on the post-peak (softening) behavior.

According to computations in Hansen et al. (1989) both the total number of ruptured bonds n_m and the density of the ruptured bonds (n_m/N) at the apex strongly depend on the specimen size. However, the magnitude of the damage variable at the apex depends only on the selected distribution of ruptured strengths as already ascertained by the expressions derived in the preceding part of this paper (Krajcinovic et al., 1993) for a parallel bar system. It is important to notice that in contrast to the parallel bar model it becomes necessary to make distinction between the density of ruptured bonds $D = (n/N)$ and the parameter ω defining the reduction of the secant modulus $K = K(1 - \omega)$. Both of these parameters, as expected, depend on the microstructure (selected distribution of the link rupture strengths $p(f_r)$). However, only the parameter ω, or more accurately the magnitude of the secant modulus $K(\omega)$, is invariant of the lattice size. Since the magnitude of the specimen (lattice) secant modulus $K(\omega)$ is readily measurable in experiments this conclusion is potentially very important for the selection of the internal variable quantifying the damage.

The other important set of conclusions in Hansen et al. (1989) concerns the post-peak or softening part of the lattice response. As indicated above the ascending segments of the rescaled force–displacement relation (7), in conjunction with (9), determined for different lattice sizes λ were found to collapse on a single master curve. A single parameter β, in conjunction with the finite-size scaling law (5) and (6), suffices to eliminate the influence of the lattice size λ, details (higher statistical momenta) of the damage distribution and microstructure (precise location of links having given rupture strengths within the lattice). The scatter of results about their means was found to be very small as well. In summary, the response of the lattice along the ascending segment of the force–displacement curve, including the apex itself, can be with acceptable accuracy estimated using the self-consistent models (or some other first-order effective continuum model).

In the pre-peak, effective continuum regime the defects (clusters of missing links) are small and far away from each other. The stress fluctuations are local and spread over a small part of the lattice. Consequently, the sequence of the link ruptures is dominated by the distribution of link strengths (de Arcangelis, 1990). Within this phase of the deformation process spatial distribution of links of different strength has a second-order effect on the response. The lattice response is local and governed by the averages of the involved fields.

The modeling of the softening response turned out to be everything but simple. The numerical results of Hansen et al. (1989) strongly suggest development of a multi-fractal force distribution at the incipient rupture of the lattice. Within the post-peak regime, characterized by significant defect densities, the stress fluctuations surrounding the defects spread over most of the lattice. Therefore, each link is subjected to a different force. The local (rather than the average) stress becomes a dominant factor of the lattice response near the point of rupture. Omitting the details, available in Hansen et al. (1989), Herrmann et al. (1989), de Arcangelis (1990) and Hansen (1990), it suffices to state that the scaling behavior of the lattice at the incipient rupture requires an infinity of exponents defining different statistical momenta of the distribution of forces in cutting links. The post-peak response preceding the lattice rupture depends on the higher statistical momenta of the initial (quenched) disorder, i.e., unlikely events. The scatter of the results in the softening regime is much more pronounced and

quite persistent. Experimental evidence of this phenomenon is well documented in the case of heterogeneous materials such as concrete (see, for example, Hegemier and Reed, 1985).

Finally, it should not be construed that the multi-fractal nature of the force distribution in links during the softening regime has anything to do with the discretization or modeling of the solid by a truss. Identical analyses performed for a grid (frame) by Herrmann et al. (1989) demonstrated identical trends leading to the same conclusions.

5. Summary and conclusions

The study presented in this two-part paper has a qualitative character. The considered discretizations are insufficiently sophisticated to provide for a rigorous and quantitative description of the behavior of brittle solids with disordered microstructure. Additionally, all considerations in this study were based on analyses of two-dimensional systems overestimating the role of the defect interactions on the macro response. Finally, all lattices considered in this study were limited in size emphasizing the size effect. Nevertheless, unencumbered by complex mathematical structure and amenable to analytical solutions and inexpensive numerical simulations the considered models are valuable in discerning the dominant and universal trends in the behavior of disordered solids.

The macro response of a solid with disordered structure during a brittle deformation process consists of three distinctly different regimes:

(a) During the initial regime, characterized by a low density of small defects scattered throughout the solid, the macro response is local. Transport parameters, such as lattice stiffness, can be computed from volume averages of defects and the size effects are readily determined using appropriate finite-size scaling. Stress fluctuations are both small and local. Owing to its effective continuum nature the hardening segments of the response of systems containing similar densities of defects are similar as well.

(b) The character of the response changes drastically in the vicinity of the elastic percolation threshold. The scaling law for the system tangent stiffness is characterized by a strongly nonlinear dependence on the proximity parameter. Yet, the self-consistent estimates of the damage and secant moduli at the percolation threshold are in *close agreement* with numerical simulations.

(c) The response in the post-peak (softening) regime depends on the higher (extreme) statistical momenta of the initial disorder and stress distribution leading to a large test-to-test scatter. Consequently, the predictions of the expected values of the ultimate rupture strength of the system are of limited utility.

From the modeling viewpoint it is important to notice that the effective continuum models (Horii and Nemat-Nasser, 1983; Krajcinovic and Sumarac, 1989; Krajcinovic, 1989; Nemat-Nasser and Hori, 1990, etc.) can be used *along the entire length of the hardening regime including the prediction of the percolation threshold* (onset of localization). If further substantiated this conclusion may render development of higher-order effective continua models unnecessary. Identifying the considered process of damage evolution as a second-order phase transition justifies application of several novel methods of statistical physics. More importantly it becomes possible to identify *universal parameters* and trends in deformation. These universal parameters are invariant with respect to discretization (lattice regularity) and details of the microstructural disorder. They are common to a wide spectrum of materials and phenomena.

At this point it seems certain that the secant stiffness modulus represents a proper choice for the internal variable quantifying accumulated damage. In the pre-peak response the secant moduli are readily measured in tests (Lemaitre and Chaboche, 1978) in addition to having attributes of universality (invariance with respect to the speciment size, dilution sequence, details of the microstructural disorder, etc.). In three-dimensional problems the stiffness tensor inherently incorporates anisotropy which is one of the criteria defining the universality group (Sengers, 1985). Finally, the damage effective continua micromechanical models (Horii and Nemat-Nasser, 1983; Krajcinovic, 1989, etc.) is also measured as

the change in the stiffness tensor. Hence, the two theories, valid for different ranges of microdefect densities, are mutually compatible.

In conclusion, the present two-part study of a set of rather primitive discrete models leads to some interesting conclusions related to cooperative phenomena in brittle deformation. The study helps to classify the mechanical damage evolution models as *second-order phase transitions* justifying application of novel statistical physics theories. The study also identifies necessary thermodynamic variables defining the state and the change of state in a deformation process dominated by microcrack evolution. Most importantly, the present study establishes *universal trends and parameters* defining critical state and behavior for the considered class of problems.

Acknowledgement

The authors gratefully acknowledge the financial support rendered by the research grants from the US Department of Energy, Office of Basic Energy Research, Division of Engineering and Geosciences and US Army Research Office, Engineering Science Division, Structures and Dynamics Branch which made this work possible.

References

Beale, P.D. and D.J. Srolovitz (1988), Elastic fracture in random materials, *Phys. Rev. B 37*, 5500–5507.

Benguigui, K. (1984), Experimental study of the elastic properties of a percolating system, *Phys. Rev. Lett. 53*, 2028–2030.

Benguigui, L., P. Ron and D.J. Bergman, (1987), Strain and stress at the fracture of percolative media, *J. Phys. 48*, 1547–1551.

Cassidy, J.J., A. Hiltner and E. Baer (1990), The response of the hierarchical structure of the intervertebral disc to uniaxial compression, *J. Mater. Sci.: Mater. Medic. 1*, 69–80.

de Arcangelis, L. (1990), Randomness in breaking thresholds, in: H.J. Herrmann and S. Roux, eds., *Statistical Models for the Fracture of Disordered Media*, North Holland, Amsterdam, pp. 229–260.

de Gennes, P.-G. (1979), *Scaling Concepts in Polymer Physics*, Cornell University Press, Ithaca, NY.

Englman, R., Z. Jaeger and A. Levi (1984), Percolation theoretical treatment of two-dimensional fragmentation in solids, *Philos. Mag. B 50*, 307–315.

Feng, S. and P.N. Sen (1984), Percolation on elastic networks: New exponent and threshold, *Phys. Rev. Lett. 52*, 216–219.

Feng, S., M.F. Thorpe and E. Garboczi (1985), Effective medium theory of percolation on central-force elastic networks, *Phys. Rev. B 31*, 276–280.

Hansen, A. (1990), Disorder, in: H.J. Herrmann and S. Roux, eds., *Statistical Models for the Fracture of Disordered Media*, North Holland, Amsterdam, pp. 115–158.

Hansen, A., S. Roux and H.J. Herrmann (1989), Rupture of central-force lattices, *J. Phys. France 50*, 733–744.

Harlow, D.G. and S.L. Phoenix (1982), Probability distributions for the strength of fibrous materials under local load sharing I: Two-level failure and edge effects, *Adv. Appl. Prob. 14*, 68–94.

Hegemier, G.A. and R.H. Reed (1985), On deformation and failure of brittle solids: Some outstanding issues, *Mech. Mater. 4*, 215–259.

Herrmann, H.J., A. Hansen and S. Roux (1989), Fracture of disordered, elastic lattices in two dimensions, *Phys. Rev. B 39*, 637–648.

Herrmann, H.J. and S. Roux (1990), eds., Modelization of fracture in disordered systems, in: *Statistical Models for the Fracture of Disordered Media*, North-Holland, Amsterdam, pp. 159–188.

Horii, H. and S. Nemat-Nasser (1983), Overall moduli of solids with microcracks: Load induced anisotropy, *J. Mech. Phys. Solids, 31*, 155–171.

Kantor, Y. and I. Webman (1984), Elastic properties of random percolating systems, *Phys. Rev. Lett. 5*, 1891–1894.

Kinzel, W. (1983), Directed percolation, *Ann. Israel Phys. Soc. 5*, 525–445.

Krajcinovic, D. (1989), Damage mechanics, *Mech. Mater. 8*, 117–197.

Krajcinovic, D. and M. Basista, (1991), Rupture of central-force lattices revisited, *J. Phys. I 1*, 241–245.

Krajcinovic, D., V. Lubarda and D. Sumarac (1993), Fundamental aspects of the brittle cooperative phenomena, *Mech. Mater. 15*, 99–115.

Krajcinovic, D. and D. Sumarac (1989), A mesomechanical model for brittle deformation processes, *J. Appl. Mech. 56*, 51–56.

Lemaitre, J. (1986), Local approach of fracture, *Eng. Fract. Mech. 25*, 523–537.

Lemaitre, J. and J.L. Chaboche (1978), Aspect phenomenologique de la rupture par endommagement, *J. Mech. Appl. 2*, 317–365.

Mandelbrot, B.B., D.E. Pasoja and A.J. Paullay (1984), Fractal character of fracture surface of metals, *Nature 308*, 1571–1572.

Nemat-Nasser, S. and M. Hori (1990), Elastic solids with microdefects, in: G.J. Weng, M. Taya and H. Abe, eds., *Micromechanics and Inhomogeneity*, Springer, New York, pp. 297–320.

Ostoja-Starzewski, M. and C. Wang (1989), Linear elasticity of